 doi:10.20944/preprints202108.0100.v1

Type of the Paper (Article)

A dansyl-modified sphingosine kinase inhibitor DPF-543 enhanced *de novo* ceramide generation

Maftuna Shamshiddinova [1#], Shokhid Gulyamov [1#], Hee Jung Kim [1], Seo Hyeon Jung [1], Dong Jae Baek [2] and Yong-Moon Lee [1, *]

[1] College of Pharmacy, Chungbuk National University, Chungbuk 28160, South Korea; shamshiddinovamaftuna@gmail.com (M.S.); shohid9395@gmail.com (S.G.); rlagmlwnd94@naver.com (H.K.); sherry987@naver.com (S.J.).

[2] College of Pharmacy, Mokpo National University, Jeonnam 58554, South Korea; dbaek@mokpo.ac.kr (D. B.)

* Correspondence: ymleefn@cbnu.ac.kr (Y.L.); Tel.: +82-43-261-2825

\# These authors contributed equally to this work.

Abstract: Sphingosine-1-phosphate (S1P) synthesized by sphingosine kinase (SPHK) is a signaling molecule, involved in cell proliferation, growth, differentiation, and survival. Indeed, a sharp increase of S1P was linked to the pathological outcome with inflammation, cancer metastasis or angiogenesis etc. In this regard, the SPHK/S1P axis regulation has been a specific issue in anti-cancer strategy to turn accumulated sphingosine (SPN) into cytotoxic ceramides (Cers). For these purposes, there have been numerous chemicals synthesized for SPHK inhibition. In this study, we investigated the comparative efficiency of dansylated PF-543 (DPF-543) on the Cers synthesis along with PF-543. DPF-543 deserved attention in strong cytotoxicity, due to the cytotoxic Cers accumulation by ceramide synthase (CerSs). DPF-543 exhibited dual actions on Cers synthesis by enhance the serine palmitoyltransferase (SPT) activity, and by inhibiting SPHKs which eventually induced an unusual environment of the high amount of 3-ketosphinganine and sphinganine (SPA). SPA in turn was consumed to synthesize Cers via de novo pathway. Interestingly, PF-543 increased only the SPN level, but not for SPA. In addition, DPF-543 mildly activates acid sphingomyelinase (aS-Mase) that contributes a partial increase on Cers. Collectively, a dansyl-modified DPF-543 relatively enhanced Cers accumulation via de novo pathway which was not observed in PF-543. Our results demonstrated that the structural modification on SPHK inhibitors is still an attractive anti-cancer strategy by regulating sphingolipid metabolism.

Keywords: PF-543; ceramide; SPHK; SPT; ceramide synthases; sphingolipid; metabolism; LC-MS/MS.

 doi:10.20944/preprints202108.0100.v1

1. Introduction

Sphingolipid metabolism initiates via the de novo synthesis pathway at the cytosolic leaflet of the ER by serine palmitoyltransferase (SPT), which catalyzes L-serine with palmitoyl-CoA in the presence of pyridoxal phosphate and forms 3-ketodihydrosphingosine (KDS) [1]. Alternately KDS reductase reduces the ketone group of KDS into hydroxyl group in a NADPH dependent manner and produces dihydrosphingosine (DHS) [2]. Subsequently six distinct ceramide synthases (CerSs) turn DHS into dihydroceramides (DHCers) by acylation [3, 4]. Formed DHCers varying on fatty acid chain length depend on which type of CerS catalyzed the reaction. For instance, CerS1 produces N-stearoyl-D-erythro-sphingosine, C18-ceramide (d18:1/18:0), CerS2 is responsible for long chain ceramides including C20-C24 [5-7].On the other hand, CerS3 prefers very long chain acyl CoAs mainly C26-ceramide, and highly expressed in the testis[8]. Unlikely CerS1, CerS4 also generates ceramides with C20-22 and alteration of CerS4 expression is highly associated with skin diseases [9-11]. Eventually, CerS5 and CerS6 produce C16-ceramide, as both have privilege towards the palmitoyl CoA as a substrate [12, 13]. Afterwards, DHCer desaturase 1/2 (DES1/2) enzymes in endoplasmic reticulum (ER) membrane converts the dihydrosphingoid bases into ceramides [14]. Formed ceramide is transported from the ER to the Golgi by vesicular transportation or via ceramide transport protein CERT [15-17]. Ceramide is a central hub in sphingolipid metabolism, which is involved in formation of complex glycosphingolipids, sphingomyelin (SM) and ceramide-1-phosphate. Another catabolic pathway of ceramide so called salvage pathway produces a bioactive signaling molecule sphingosine-1-phosphate (S1P)[18]. Ceramide eventually catabolized to sphingosine by three different Ceramidases, which are classified by their pH optima[19]. Sphingosine kinase (SPHK) enzymes phosphorylate the 1-hydroxyl group of sphingosines and produces S1P. There are two isoforms of SPHK were found in mammals: SPHK1 is localized in cytoplasm and SPHK2 is found in nucleus[20]. SPHK/S1P axis is actively involved in cell survival, proliferation, cancer metastasis, inflammation, type II diabetes, cardiovascular diseases[21, 22]. SPHK is overexpressed in hyperproliferative diseases, and its metabolite S1P progresses cancer cell proliferation and metastasis[21]. Thus designing potential therapeutic chemicals which regulate SPHK/S1P signaling pathway became the trending topic among the scientists. Myriads of SPHK selective inhibitors were designed and applied into clinical trials. For example, Fingolimod (FTY720) SPHK1 selective inhibitor is widely used as an anti-sclerotic drug activates protein phosphatase 2A and suppresses cancer cell growth[23]. PF-543 is the most potent SPHK 1 inhibitor with a nonlipid structure designed by Pfizer Co. Inspite of high inhibitory activity (IC_{50} 2.0nM), this compound demonstrated low efficacy in certain types of cancer cell lines, possibly due to the accumulated cellular sphingoid bases[24]. PF-543 treatment lowered the SPHK1 expression on Ca9-22 and HSC-3 cells, and decreased cell proliferation in a time- and dose-dependent manner. Furthermore long term incubation caused the induction of autophagy and prevented the necrotic cell death[25]. In vivo application of PF-543 improved the symptoms and pathological changes in dextran sodium sulfate induced ulcerative colitis in murine models. Moreover, it showed anti-inflammatory

Preprints (www.preprints.org) | NOT PEER-REVIEWED | Posted: 4 August 2021 doi:10.20944/preprints202108.0100.v1

response by depleting the level of IL-1b and IL-6 [26]. Various inhibitors were designed based on the core structure of PF-543 to refine its anticancer efficacy.

Fluorophore labeled PF-543 analogue BODIPY-PF-543 gave the same SPHK1 inhibition efficacy as PF-543, by showing the IC_{50} values 19.92 and 11.24 nM, respectively. Confocal microscopy results proved that BODIPY-PF-543 was mainly located in the cytosol of the cells after treatment and might be useful for cell imaging [27]. For visualizing the local distribution of PF-543, DPF-543 was synthesized by labeling PF-543 structure with 5-(dimethylamino) naphthalene-1-sulfonyl (Dansyl) moiety and recommended to utilize also for fluorescent-based SPHK assays (Fig. 1a). In the SPHK1 inhibition assay, PF-543 and DPF-543 have similar IC_{50} value, 10.4±3.2 nM and 12.3±2.5 nM, respectively and docking study confirmed the DPF-543 have the same binding pattern to SPHK1 likewise PF-543[28]. In this report, we investigated the comparative study on the effects of local structural modification on PF-543 on the sphingolipid metabolism. Especially, we focused on the relative changes of dihydroceramides (DHCers) and ceramides (Cers) distribution because PF-543 makes a local environment on the transient SPHK substrates accumulation of cellular sphingoid bases by inhibiting SPHK1. The LC-MS/MS system was used to analyze DHCers and Cers in the LLC-PK1 cells, a porcine kidney epithelial cells which have been used for sphingolipid metabolism research.

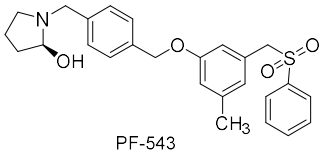

PF-543

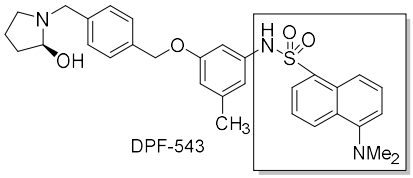

DPF-543

Fig.1. Structure of PF-543 and DPF-543

2. Results

2.1. Cytotoxicity of DPF-543

In LLC-PK1 cells, the DPF-543 and PF-543 were not toxic in the tested concentration below 31.25 μM (Fig. 2). The dansyl derivatization on the position far from an active site in PF-543 showed more cytotoxic effect. The cytotoxicity by DPF-543 was observed predominantly from 62.5 μM. From this concentration, the cell viability by DPF-543 begin to be reduced to 74% while PF-543 treatment was still viable showing 96% viability. The maximum gap between DPF-543 and PF-543 on the cell viability was observed when 125μM of DPF-543 or PF-543 had been tested. Under the 500 μM or higher concentration, two chemicals gave the irreversible toxicity with 5% cell viability. For further experiments on the sphingolipid metabolism and related enzyme assays, PF-543 and DPF-543 below 30.0 μM were applied to the cells.

Preprints (www.preprints.org) | NOT PEER-REVIEWED | Posted: 4 August 2021 doi:10.20944/preprints202108.0100.v1

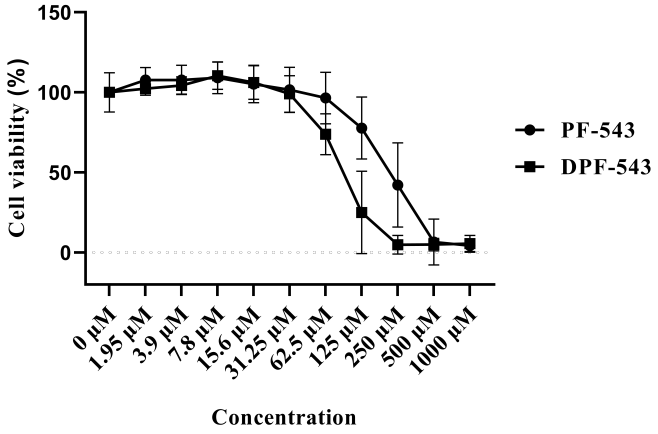

Fig.2. Cell viability of PF-543 and DPF-543 in LLC-PK1 cells

2.2. DPF-543 activates SPT *in vitro*

The DPF-543 and PF-543 have displayed the specific sphingosine kinase (SPHK) inhibition [28]. To clarify a DPF-543 cytotoxic effect, we designed to look at the first step of sphingolipid biosynthesis initiated by serine-palmitoyl transferase (SPT). The SPT activity was measured by tracing the two deuterium (2D-) labelled sphingolipid metabolites, 3-keto sphinganine (2D) and sphinganine (2D). In these conditions, endogenous sphingolipid metabolites were also measured simultaneously. The DPF-543 treatment triggered the 3-keto sphinganine (2D) production, which was not observed by PF-543 treatment (Fig. 3a). The sphinganine (2D) increase by DPF-543 reconfirmed that DF543 activates the SPT enzyme to synthesize newly initial sphingolipid metabolites, which may produce cytotoxic sphingolipid metabolites such as ceramides. In the same condition, endogenous 3-keto sphinganine (3-KDS) and sphinganine (SPA) were significantly observed after DPF-543 treatment (Fig.3b). Indeed, the DPF-543 treatment showed the 4-folds increases of 3-KDS(D2) and SPA(D2), which also provided the parallel relation to the increase of endogenous sphingolipid metabolites. Interestingly, the PF-543 treatment greatly increased the sphingosine (SPN), a metabolite from the ceramide salvage pathway by blocking SPHK activities. Practically, PF-543 treatment showed almost 6-folds SPN accumulation from 13 pmol/mg protein to 75 pmol/mg protein.

(a)

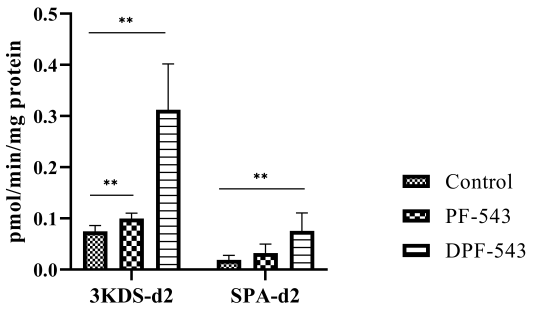

Preprints (www.preprints.org) | NOT PEER-REVIEWED | Posted: 4 August 2021 doi:10.20944/preprints202108.0100.v1

(b)

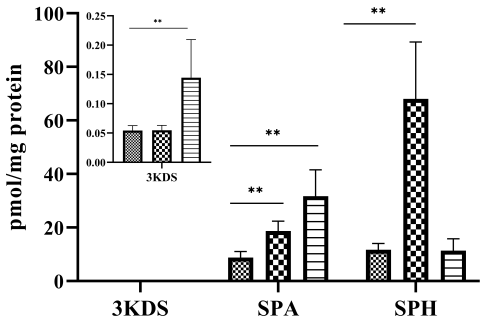

Fig.3. (a) deutralized 3KDS and SPA accumulation by PF-543 and DPF-543; (b) PF-543 and DPF-543 impact on endogenous sphingoid bases

2.3. DPF-543 strongly activates CerSs

C17-sphinganine was used as a specific substrate on CerSase activity. We exogenously spiked palmitoyl-CoA into reaction mixture as a fatty acid resource, thus palmitoyl (C16:0) Ceramide (C17 sphingoid base) was profoundly formed. Total increased amount of C17 based DHCers (C17-DHCers) were from 8.75 nmol/mg protein to 9.34 nmol/mg protein by PF-543 and 18.07 nmol/mg protein by DPF-543, relatively (Fig. 4a). Next, we investigated the relative increases on individual C17-DHCers. The abundant C17-DHCers in LLC-PK1 cells were C17-DHCer with FA 16:0 (2952.7 pmol/mg protein) or 18:1 (5398.1 pmol/mg protein). Overall, PF-543 treatment did not greatly induce the C17-DHCer synthesis. Unexpectedly, the dansyl modified DPF-543 treatment significantly raised the both content of C17-DHCers 16:0 and 18:1 for 1.75 and 2.1 folds, respectively. Even though C17-DHCer with FA chain 18:0, 20:0 and 22:0 had a slight increase by PF-543, there was almost two-fold augmentation in other C17-DHCers (18:0, 20:0 isomer, 22:0 isomer) by DPF-543. By DPF-543 treatment, the most fold- increase was observed in C17-DHCer 24:1, 24:0 and its isomers, 4-fold, 6.6 and 9.5 folds, respectively. On the contrary, the content of C17-DHCer 22:0 was not altered significantly (Fig. 4b).

The DHCer desaturase is a responsible enzyme to convert the increased DHCers by DPF-543 into Ceramides (Cers). As the C17-DHCers were the specific substrate for DHCer desaturase, we determined the newly synthesized C17-Cers. Comparing to the increased amount of C17-Cers (72 pmol/mg protein) in control groups, The PF-543 or DPF-543 treatment demonstrated the higher DHCer desaturase activities on C17-Cers synthesis by the total Cer 2.55 and 5.36 folds increases, respectively(Fig. 4c). The Cer with fatty acid chain 16:0 and 24:0 was the major ceramides synthesized by DPF-543 treatment. Unexpectedly, the synthesis of C17-Cer 18:1 was not effectively converted from C17-DHCer 18:1, which has been a major C17-DHCer, by DPF-543 (Fig. 4d). The result from DPF-543 application to the effectiveness on the new Cers synthesis was postulated that the relatively low conversion ratio by DHCer desaturase may be connected to prevent the excessive increase of cytotoxic Cers in a short period (Supplementary table 3).

Preprints (www.preprints.org) | NOT PEER-REVIEWED | Posted: 4 August 2021 doi:10.20944/preprints202108.0100.v1

(a)

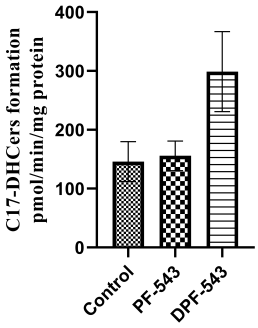

(b)

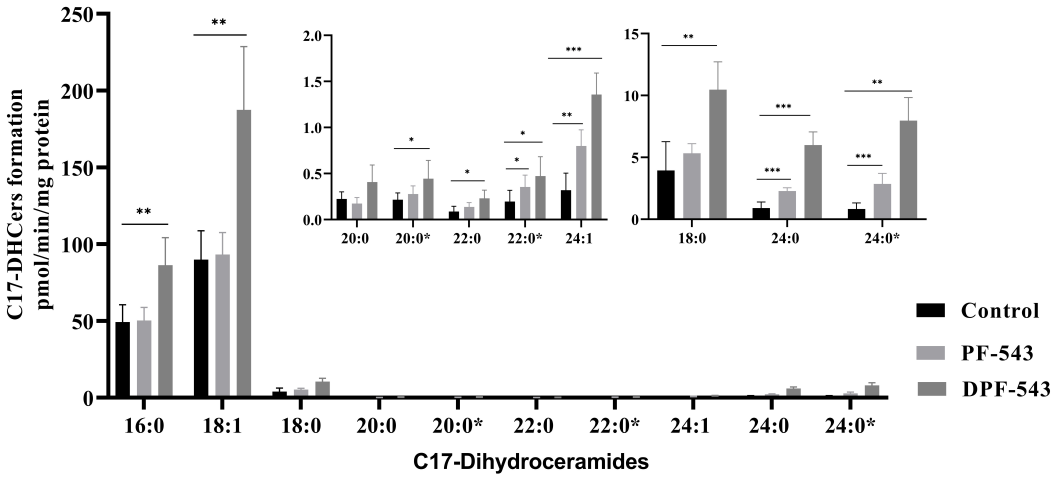

(c)

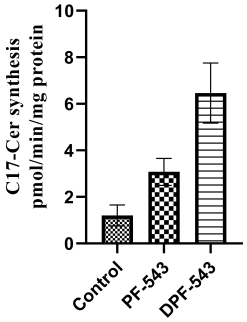

(d)

Preprints (www.preprints.org) | NOT PEER-REVIEWED | Posted: 4 August 2021 doi:10.20944/preprints202108.0100.v1

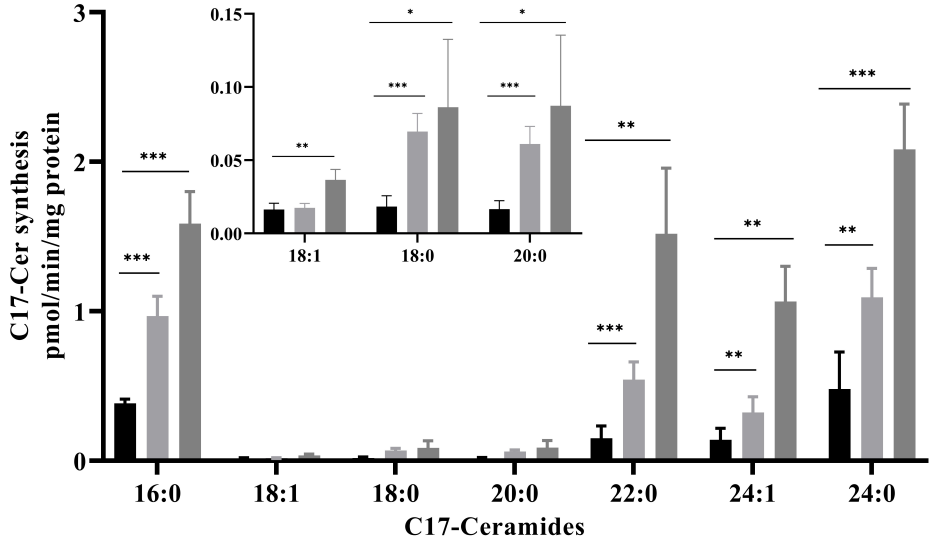

Fig.4. (a) Total C17-DHCer amount in PF-543 and DPF-543 application; (b) Individual C17-DHCer accumulation by PF-543 and DPF-543 treatment; (c) Total C17-Cer amount in PF-543 and DPF-543 application; (d) Individual C17-Cer alteration by PF-543 and DPF-543

2.4. DPF-543 activates aSMase

Next, we considered the activation of another Cers synthetic route by aSMase. The PF-543 or DPF-543 also activated aSMase to produce fluorescent phosphocholine directly from sphingomyelin (SM) hydrolysis in this assay kit (Fig. 5). The aSMase activity by DPF-543 was 1.5-fold higher than control level. The simultaneous increase of total endogenous Cers by DPF-543 were also observed (Fig. 6a). The accumulation of total Cers was a sum both from de novo and from aSMase route. Of most importance, the distribution pattern of endogenous Cer analogs by DPF-543 exhibited a closed similarity on the accumulation pattern by C17-sphinganine spiking test demonstrated on Fig.4d. The endogenous Cer18:1 amount were observed relatively low which was also the low synthetic rate of C17-Cer18:1 in the environment of highly accumulated C17-DHCer 18:1 by DPF-543 (Fig. 6b).

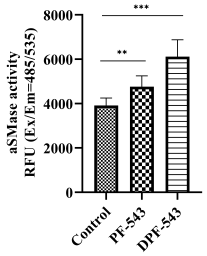

Fig.5. Acid sphingomyelinase activation by PF-543 and DPF-543 treatment

(a)

Preprints (www.preprints.org) | NOT PEER-REVIEWED | Posted: 4 August 2021 doi:10.20944/preprints202108.0100.v1

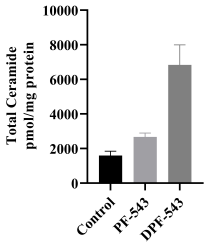

(b)

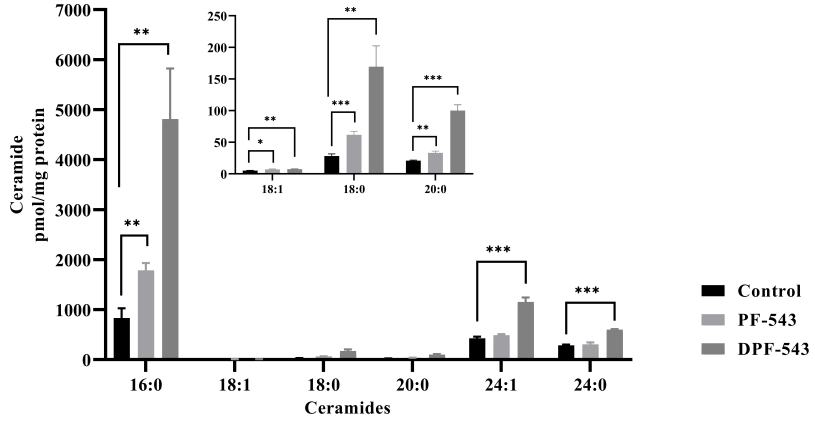

Fig.6. (a) Total endogenous Ceramide accumulation by SPHK1 inhibitors; (b) Alteration of endogenous Ceramides by SPHK1 inhibitors

2.5. DPF-543 activates Cer synthesis via de novo pathway

A strong SPT inhibitor, 10 uM myriocin (Myr) treatment reduced almost 50 % the endogenous Cers compared to control. However, PF-543 and DPF-543 application with Myr triggered the Cers accumulation by roughly 3.5 and 10.4 times higher than Myr itself. By comparing the data of total Cers amount by DPF-543 (Fig 6a and Fig. 7a), the inhibitory contribution of Myr in Cer synthesis was not so higher than expected (8.5 % Cers reduced by myriocin). The relative distribution of each Cers by Myr plus DPF-543 were similar to DPF-543 single treatment (Fig. 7b). The accumulated Cers by DPF-543 might be contributed from via another de novo route or aSMase route.

(a)

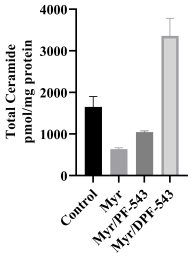

(b)

Preprints (www.preprints.org) | NOT PEER-REVIEWED | Posted: 4 August 2021 doi:10.20944/preprints202108.0100.v1

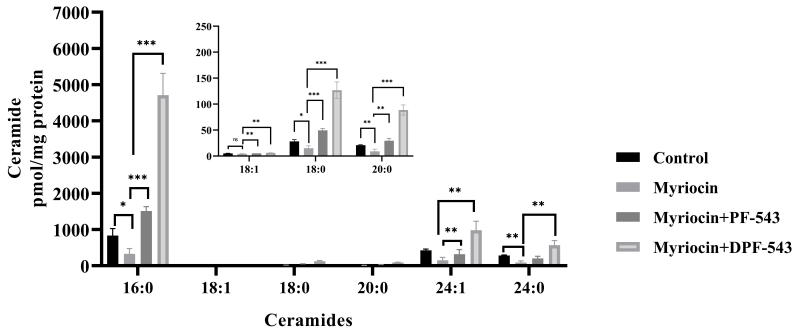

Fig.7. (a) PF-543 and DPF-543 impact on total ceramide accumulation reduced by myriocin treatment; (b) Alteration of individual ceramides by PF-543 and DPF-543 after myriocin treatment

Therefore, a strong CerS inhibitor fumonisin B1 (FB1 35 uM) was applied to know whether DPF-543-induced Cers accumulation is regulated or not. As shown in Fig. 8a, FB1 treatment declined almost half amount of total Cers by DPF-543, indicating that CerSs were highly activated by DPF-543 although a part of the conversion from sphinganine (SPA) to DHCers were inhibited by FB1 treatment. The Cers distribution pattern by FB1 was almost same to the data obtained by myriocin treatment, except the half-reduction on Cers amount (Fig. 8b). Finally, we re-confirmed the de novo steps by combined treatment of myriocin and FB1 during the PDF543 activation on the Cer synthesis.

(a)

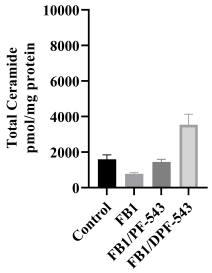

(b)

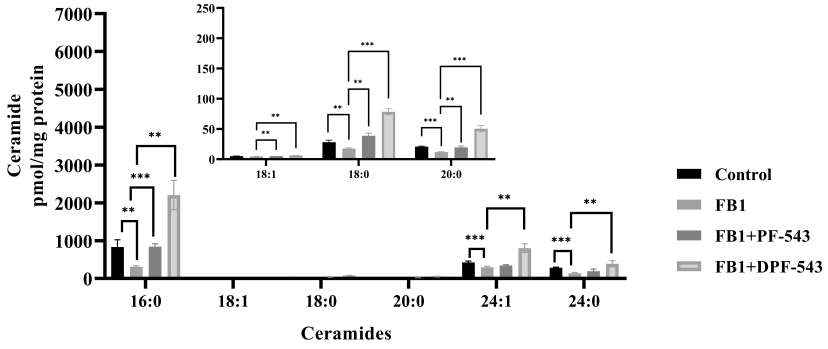

Preprints (www.preprints.org) | NOT PEER-REVIEWED | Posted: 4 August 2021 doi:10.20944/preprints202108.0100.v1

Fig.8. (a) PF-543 and DPF-543 impact on total ceramide accumulation reduced by FB-1 treatment; (b) Alteration of individual ceramides by PF-543 and DPF-543 after FB-1 treatment

The total Cer amount after combined treatment was almost the same to Figure 8a, indicating the contribution of SPT activity on DPF-543-induced Cer synthesis was negligible (Fig. 9a). Likewise, the Cers amount and distribution by myriocin plus FB1 treatment showed the almost similar Cers pattern obtained from FB1 treatment (Fig.9 b). In our experiment, DPF-543, a PF-543 structure modified at dansylated moiety at sulphonyl position enhanced the Cer synthesis via not only aSMase activation but also strongly CerSs activation which has a responsible role for DHCers formation needed for Cer synthesis.

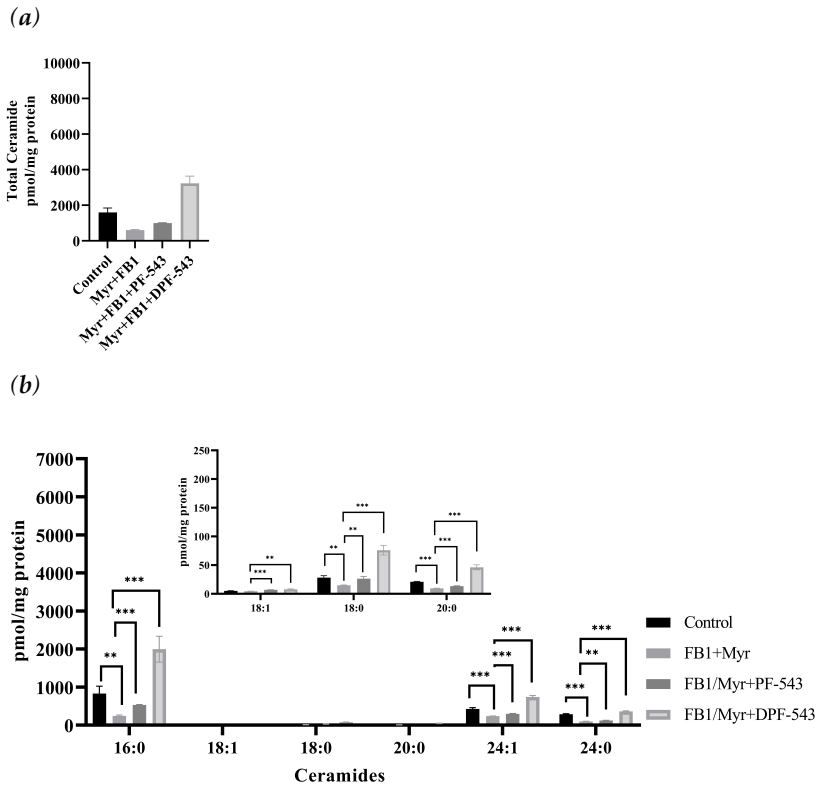

Fig.9. (a) PF-543 and DPF-543 impact on total ceramide accumulation mitigated by combined treatment of myriocin with FB-1; (b) Alteration of individual ceramides by PF-543 and DPF-543 after combined treatment of myriocin with FB-1

3. Discussion

SPHK1 expression and S1P formation was highly elevated in a variety of tumors such as ovarian, breast, lung, colorectal and prostate cancers, and hepatocellular carcinoma. For instance, overexpression of SPHK1 in a xenograft model of ovarian cancer enhanced tumor growth, following by enhancement of proliferation and stemness[29]. Thus, SPHK1/S1P axis regulation became one of the main targets in cancer

Preprints (www.preprints.org) | NOT PEER-REVIEWED | Posted: 4 August 2021 doi:10.20944/preprints202108.0100.v1

treatment. Up to date, a wide range of sphingosine, amidine, bicyclic aryl, amino alcohol based and lipidic and non-lipidic small molecule SPHK inhibitors were designed and applied into the area of cancer, allergy and inflammation, transplantation and viral infection treatment[30].

Dansylation of PF-543 structure was performed by labeling core structure with 5-(dimethylamino)naphthalene-1-sulfonyl and as dansyl group has fluorescence property it was recommended to utilize for fluorescent-based SPHK activity assays. SPHK1 inhibition assay showed that, PF-543 and dansyl-PF-543 both have almost the same binding affinity and binding pattern to SPHK1[28]. The (R)-2-(hydroxymethyl)-pyrrolidine group of PF-543 is terminal-1 bound substrate and replaces the position of a lipid head group. The pyrrolidine nitrogen and the hydroxyl of PF-543 forms hydrogen bonds to the sidechain of Asp264 which is involved in sphingosine recognition. PF-543 was reported as a weak substrate for SPHK1. To phosphorylate the PF-543 structure, (R)-2-(hydroxymethyl)- pyrrolidine head group need to be rotated for 180° to move the primary hydroxyl into a position of the lipid primary hydroxyl group. As SPHK2 has three residue differences in the lipid binding site compared to SPHK1. Cys is in the position of Phe374, Val replaces the Ile260 and Lue is Met358 in SPHK2. Those differences made binding site larger in SPHK2. The phenyl ring of PF-543 binds against Phe374 may be the tightest bound part of the molecule. Thus, Cys374 in SPHK2 may be a significant reason ~132-fold selectivity of PF-543 for SPHK1 over SPHK2[31].

In vitro application of PF-543 in some cells lead to autophagy and necrosis. For instance, the survival rate of Ca9-22 and HSC-3 cells diminished to 19.8% and 26.7% respectively in the presence of 25 μM PF-543. The morphology of above-mentioned cells were also affected by PF-543 treatment[25]. In case of HTC-116 cells, PF-543 time and dose dependently displayed anti-survival effect, which was revealed after 48-hour incubation with 10μM concentration of chemical[32].

The CCK-8 reagents have higher aqueous solubility than the other tetrazolium salts such as MTT, XTT, MTS or WST, this cell viability kit was highly recommended for cell cytotoxicity, viability, and proliferation tests [33, 34]. Although the dansylation on PF-543 provides considerable merits on the experimental visualization and simplicity for bioassay, the larger molecular weight and hydrophobicity in DPF543 might be related to enhance the membrane permeability and to stay longer in the cells to trigger the cytotoxicity. Fortunately, the dansyl modification on PF-543 (DPF-543) far from the position of SPHK binding site did not reduce its activity [28]. Previously, PF-543 was reported not directly activate the CerSases which is an essential enzyme to produce Cers [24]. The higher cytotoxicity of DPF-543 may come from the strong potency to the production of Cers. DPF-543 showed almost 5-time stronger cytotoxicity on LLC-PK1 cells than its prototype.

There were several examples on the regulation for Cer synthesis by SPHK inhibitors. N,N-dimethylsphingosine (DMS) induces apoptosis in hematopoietic and carcinoma originated cancer cells by sphingosine 1-phosphate (S1P) reduction. This changed the ceramide/SPP rheostat in favor of cellular ceramide, which induced apoptotic progress in

 doi:10.20944/preprints202108.0100.v1

cancer cells [35, 36]. The SPHK regulation has been investigated as a drug target for anticancer therapy motivated to design the selective SPHK inhibitors, F-12509, ABC294640, SKI-I, K145 and SKI-II[37-42]. The SPHK inhibitor in general not only reduced S1P but also simultaneously increased Cers. For example, the human gastric cancer HGC 27 cells treated with SKI II revealed reduced S1P levels and increased amounts of DHCers and Cers. The DHCer accumulation was remained for 48 hours, whereas Cers level went to basal level within 24 hours [42].

In our results, the enhancement of hydrophobicity by dansylation on PF-543 gave a great enhancement on CerSases activities resulting endogenous Cers increase via de novo sphingolipid pathway (Fig. 6A). In this CerSase assay, the Cers conversion from DHCers by DHCer desaturase inserting a double bond on C4-C5 position of sphingoid bases was shown the inefficient conversion ratio. Most of conversion ratio of Cers from DHCers were far below 100%, indicating the desaturation process is an inefficient and thus a rate-limiting step to produce the Cers (Supl. Table 4). Nevertheless, the conversion ratio on long chained Cers of C22:0 and C24:1 was relatively higher in DPF-543 treatment, which raised the DHCers by CerSases activation. Compare to the Cers increase by PF-543, DPF-543 selectively at least two-fold Cers increase of C22:0 and C24:1, which might reflect a stronger cytotoxicity of DPF-543.

There is evidence that lysosomal aSMase plays an important role in ceramide formation after stimulation with chemotherapeutic agents, luteolin or fluphenazine[43, 44]. Here, although the aSMase activation is not so strong, PF-543 and DPF-543 also triggered the lysosomal aSMase activation indicating the increased cytotoxicity via pro-apoptotic Cers accumulation by sphingomyelin (SM) hydrolysis (Fig. 5). In the same conditions, DPF-543 induced almost 4-fold Cers accumulation where PF-543 just showed 1,5-fold Cers increase suggesting that the Cers increase by DPF-543 might be a combined pool not only from aSMase activation but also from additional de novo synthetic pathway (Fig. 6A). Most of endogenous Cers was greatly highly accumulated by DPF-543, which increased toxicity comes from dansylation of PF-543, increased hydrophobicity and both activations of aSMase and CerSases in de novo pathway(Fig 6B).

Comparing to PF-543 effects, DPF-543 preferentially activates de novo pathway in total Cers accumulation. We further investigated whether DPF-543 could increase the Cers amounts during co-treatment of SPT inhibitor Myr or CerSs inhibitor FB1. As expected, the pretreatment of 10 uM Myr, which is a high concentration to block the SPT activity reduced total Cers amount which may be synthesized from de novo pathway. PF-543 act likely to restore Cers concentration to control level (Fig. 7A), which was similarly observed when FB1 application reduced Cers levels (Fig. 8A). The DPF-543 effect with Myr or FB1 pretreatment on the total Cers was evidently stronger than the case of PF-543. The reason of unexpected Cers increase by DPF-543 may be explained that DPF-543 stay longer in hydrophobic cellular organs including the ER membrane where de novo sphingolipid biosynthesis started with SPT activation. Another hypothesis on the S1P reduction by SPHK inhibition by DPF-543 caused a sharp change on Cer/S1P rheostat balance.

 doi:10.20944/preprints202108.0100.v1

Taken together, DPF-543 treatment strongly activated a series of enzymes located in de novo sphingolipid pathway. Although these effects on Cers accumulation is not fully explained yet, the pharmacological ability for SPA accumulation by different SPHK inhibitors is a key component to explain their different cytotoxicity. In our study, the structural design on dansylation of PF-543 with a higher hydrophobicity provided the stronger cytotoxicity caused by Cers accumulation mainly by SPA induced CerSs activation.

4. Materials and Methods

Materials

Ceramide standards with different carbonyl chain of 16, 17, 18:1, 18, 24, 24:1 were obtained from Matreya LLC (State College, PA, USA). C17-sphinganine (C17-Sa), fumonisin B1 (FB1), were purchased from Cayman Chemical (Ann Arbor, MI, USA). Myriocin and other reagents for SPT assay were from Sigma Aldrich (St. Louis, MO, USA)). PF-543 were obtained from Echelon biosciences (Salt Lake City, UT, USA). DPF-543 was synthesized from Mokpo University and evaluated as a sphingosine kinase (SPHK) inhibitor[28]. Other organic solvents were purchased from Honeywell Burdick&Jackson (Charlotte, North Carolina, US). The reagents for cell culture media were purchased from HyClone (South Logan, UT, USA). Primary antibodies of serine palmitoyltransferase long chain base subunit 1 (Sptlc1), ceramide synthase 4 (CerS4), and CerS6, and horseradish peroxidase (HRP) labeled secondary antibodies were from Thermo (Waltham, MA, US). The β-actin antibody was from Merk Millipore (Burlington, MA, USA). Sphingomyelinase (SMase) activity kit was from Abcam (Cambridge, MA, USA). Fatty acid free BSA, BSA fraction V and protease inhibitor cocktail were purchased from Roche (Mannheim, Germany). The isotope-labeled L-serine (3,3-d2) was purchased from Cambridge Isotope Laboratories, Inc (Tewksbury, MA, USA).

Cell culture

A porcine kidney proximal tubule cell line, LLC-PK1 cells were cultured in Dulbecco's Modified Eagle's medium. A human kidney proximal tubular cell HK-2 cells were in RPMI medium. Each cell was subcultured and was supplemented with 10% fetal bovine serum (FBS) and antibiotics of 100 units/mL of penicillin, and 100 ug/mL of streptomycin (P/S). The cells were grown at 37°C in a 5% CO_2.

Cell viability test

Ten thousands LLC-PK1 cells were seeded onto 96-well plate and cultured for 24 hrs in 200μL of DMEM with 10% FBS plus P/S. Standard stock solutions of PF-543 and DPF-543 (40 mM in DMSO) were diluted serially with DMSO in the range from 1000μM to 1.95μM. Grown cells were treated with each 1μL of PF-543 or DPF-543 solutions after changing the old media with fresh one (100μL). After cells were incubated for 24 hrs, cultured media was removed by gentle aspiration and replaced with 100μL of PBS. 10 μL of cell counting kit-8 (CCK-8) solution (Dojindo molecular technologies Inc.,

Preprints (www.preprints.org) | NOT PEER-REVIEWED | Posted: 4 August 2021 doi:10.20944/preprints202108.0100.v1

Rockville, MD, US) was spiked into each well. Plates were incubated for 3 hrs at 37°C for completing the orange color of formazan production on living cells. Plates were read with a microplate reader, absorbance at 450 nm.

Regulation of sphingolipid metabolism

To investigate PF-543 and DPF-543 effects on SPT activity, 10 μM of myriocin was spiked to LLC-PK1 cells and were incubated for 24 hrs before PF and DPF-543 treatment. LLC-PK1 cells were treated with either 20μM PF-543 or DPF-543. In control, the same volume of DMSO was spiked to the cells. Cells were incubated for additional 24 hrs before harvest.

To study PF-543 and DPF-543 effects on CerSs activity, 35 μM FB1 was spiked to the cells and incubated following the same protocol as noted above.

Lipid extraction

Under the 200μL of RIPA lysis buffer with complete protease inhibitor cocktail, harvested cell pellets were homogenized. Protein amount was determined according to manufacturer instruction of Thermo protein assay kit (Pierce, IL, USA). Five hundred pmol of internal standard C18:1/C17 Ceramide and 750 μL of MeOH:$CHCl_3$ (2:1, v/v) were added into 100 μg of protein lysate. The mixture incubated for overnight at 48°C. After cooled down to ambient temperature, 75μL of 1M KOH in MeOH was used for complete lipid digestion for 2-hour at 37°C with vigorous shaking. We spiked acetic acid for mixture neutralization. The mixture (750 μL) was transferred into new tubes. For lipid extraction, 350 μL of $CHCl_3$ and 150 μL of distilled water were added and vortexed, centrifuged for 5 min at 14000 rpm. Aqueous phase was re-extracted with additional $CHCl_3$. Combined lower organic phases were dried. Dried residues were reconstituted with MeOH for introducing mass spectrometry.

SPT activity

SPT activity assay was carried out in LLC-PK1 cells as reported previously with patrial modification. The assay mixture composition was a solution of 100 mM HEPES, pH 8, 5 mM DTT, 50 μM PLP, 100 μM Pal-CoA, 10 mM 3,3-D2-serine and the complete protease inhibitor cocktail[45]. The SPT assay started by adding cell lysates of 200 μg of protein into 200 μL of assay mixture, incubated at 37°C for 30 min. After the stop solution (CHCl 3 : MeOH (2:1); 500 μL) added, 50 pmol of C17-sphingosine was spiked as an internal standard for chromatographic separation and quantitation. The tubes vortexed vigorously for 5 min, centrifuged for 5 min at 14000 rpm. Lower organic phase with additional 200 μL of $CHCl_3$ were combined and dried.

CerS activity

The assay mixture contained 50 mM HEPES-KOH, pH 7.4, 25mM KCl, 2 mM $MgCl_2$, 0.5mM DTT, 0.1% fatty-acid free BSA, 50 μM Pal-CoA and 10 μM C17-sphinganine[46]. The cell lysate of 100 μg of protein was incubated at 37°C for 1 hour with 200 μL of assay mixture. Reaction was terminated by 500 μL of $CHCl_3$:MeOH (2:1; v/v) stop solution.

Preprints (www.preprints.org) | NOT PEER-REVIEWED | Posted: 4 August 2021 doi:10.20944/preprints202108.0100.v1

The tube containing newly synthesized C17 based ceramide was vortexed and centrifuged for 5 min at 14000 rpm. Lower organic phase with additional 200 µL of $CHCl_3$ extract were combined and dried.

aSMase activity

The aSMase activity assay was measured by fluorometric SMase assay method (Abcam) followed the manufacturer's protocol. The LLC-PK1 cells were incubated with 20 µM of PF-543 and DPF-543 for 24 hours. The supernatant from the cell lysate was transferred into new tube. The final volume 50 µL containing 50µg protein was loaded into 96 well plate. Then 50 µL of sphingomyelin (SM) solution was applied, the plate was incubated at 37°C for 3 hrs. After the 50 µL of red indicator for SMase product was spiked to each wells. The plate protected from light kept at ambient temperature for 2 hrs. Fluorescence intensity was measured on a microplate reader at Ex/Em 485/535 nm. The significance of relative fluorescence unit (RFU) values was calculated by ANOVA.

Immunoblotting

For immunoblotting to the expression of sphingolipid metabolic enzymes, human proximal tubule epithelial HK-2 cells were used. The collected HK-2 cells were washed twice in ice-cold PBS solution and lysed in 200µL of RIPA lysis buffer (25 mM Tris•HCl pH 7.6, 150 mM NaCl, 1% NP-40, 1% sodium deoxycholate, 0.1% SDS). The BCA protein assay kit (Thermo, Pierce, IL, USA) was used to determine protein concentration. The loaded samples containing 20 µg / 10µL protein concentration was separated on a 10% SDS-PAGE gel and transferred to PVDF membranes by semi-dry method. Then blotting status was checked by using Ponceau S reagent, membranes were washed with TBST three times for 10 minutes. The membranes were blocked in 5% BSA in TBST for overnight and then incubated with the primary anti-Sptlc1, CerS4 and CerS6 antibodies (1:1000 dilution in 5% BSA-TBST) for overnight at 4°C. Anti β-actin clone c4 mouse monoclonal antibody was prepared in 1:10000 dilution. After incubation, the membranes were washed with TBST three times for 10 minutes. The blots were then incubated for overnight with secondary horseradish peroxidase-conjugated goat anti-Rabbit IgG antibody (1:5000 dilution in 5% BSA in TBST) and goat anti-Mouse IgG (H+L) antibody (1:25000 dilution in 5% BSA in TBST) to detect targeted proteins and β-actin, respectively. The membranes were then washed three times with TBST. The protein bands were visualized by Pierce ECL Plus Western Blotting Substrate and read in Amersham Imager 600 (GE Healthcare Bio-Sciences AB, Sweden). Data was represented in Supplementary Fig.1.

LC-MS/MS conditions

AB Sciex QTRAP 4500 model mass spectrometry coupled with Shimadzu UPLC system was applied to determine the amounts of ceramides. Mass spectrometry was operated in positive ion mode. Precursor and product ions were displayed in Supplementary table 1 with optimal parameters. Linear calibration curves were constructed by using the area ratio of standard ceramides to IS C17-ceramide was used

 doi:10.20944/preprints202108.0100.v1

to build calibration curves. Each Cers were well separated on Shiseido Capcell Pak C18 MG III type, 50x3 mm, 5μM. Mobile phase A was 10 mM ammonium acetate in water with 0.1% formic acid and mobile phase B was 10 mM ammonium acetate in acetonitrile:2-propanol (4:3;v/v) with 0.1% formic acid. Gradient elution with a flow rate 0.3 ml/min, was starting 85% of B, increasing to 100% B after 1.5 min and holding for 10 min, then re-equilibrating to 85% B for 5 min. The mass spectrometry parameters for C17-Cers and C17-DHCers and other sphingolipid metabolites were listed in Supplementary Tables 2 and 3, respectively.

Supplementary Materials: The following are available online at www.mdpi.com/xxx/s1, Figure S1: Western blots of enzymes related to de novo Cers synthesis in HK-2 cells, Table S1: QTRAP 4500 mass spectrometer setting for C18:1 Ceramide analysis.

Author Contributions: Conceptualization, D.B. and Y.L.; methodology, M.S. and S.G.; formal analysis, H.K. and S.J.; investigation, M.S.; resources, S.G.; data curation, M.S.; writing—original draft preparation, M.S.; writing—review and editing, D.B. and Y. L.; visualization, M.S.; supervision, Y.L. All authors have read and agreed to the published version of the manuscript.

Funding: These results were supported by “Regional Innovation Strategy (RIS)" through the National Research Foundation of Korea (NRF) funded by the Ministry of Education (MOE).

Institutional Review Board Statement: Not applicable

Informed Consent Statement: Not applicable

Data Availability Statement: Not applicable

Acknowledgments: These results were supported by “Regional Innovation Strategy (RIS)" through the National Re-search Foundation of Korea (NRF) funded by the Ministry of Education (MOE).

Conflicts of Interest: The authors declare no conflict of interest.

Abbreviations

aSMase Acid sphingomyelinase

Cers Ceramides

CerS Ceramide synthase

CERT Ceramide transport protein

DES1/2 Desaturase ½

DHCers Dihydroceramides

DHS Dihydrosphingosine

DPF-543 Dansylated PF-543

ER Endoplasmatic reticulum

FA Fatty acid

FB1 Fumonisin B1

KDS 3-ketodihydrosphingosine

 doi:10.20944/preprints202108.0100.v1

Myr Myriocin

PalCoA Palmitoyl Coenzyme-A

PLP Pyridoxal phosphate

SPA Sphinganine

SPHK Sphingosine kinase

SM Sphingomyelin

SPN Sphingosine

SPT Serine palmitoyl transferase

S1P Sphingosine-1-phosphate

References

1. Mandon, E.C., et al., *Subcellular localization and membrane topology of serine palmitoyltransferase, 3-dehydrosphinganine reductase, and sphinganine N-acyltransferase in mouse liver.* J Biol Chem, 1992. **267**(16): p. 11144-8.
2. Beeler, T., et al., *The Saccharomyces cerevisiae TSC10/YBR265w gene encoding 3-ketosphinganine reductase is identified in a screen for temperature-sensitive suppressors of the Ca2+-sensitive csg2Delta mutant.* J Biol Chem, 1998. **273**(46): p. 30688-94.
3. Pewzner-Jung, Y., S. Ben-Dor, and A.H. Futerman, *When do Lasses (longevity assurance genes) become CerS (ceramide synthases)?: Insights into the regulation of ceramide synthesis.* J Biol Chem, 2006. **281**(35): p. 25001-5.
4. Lahiri, S., et al., *Kinetic characterization of mammalian ceramide synthases: determination of K(m) values towards sphinganine.* FEBS Lett, 2007. **581**(27): p. 5289-94.
5. Venkataraman, K., et al., *Upstream of growth and differentiation factor 1 (uog1), a mammalian homolog of the yeast longevity assurance gene 1 (LAG1), regulates N-stearoyl-sphinganine (C18-(dihydro)ceramide) synthesis in a fumonisin B1-independent manner in mammalian cells.* J Biol Chem, 2002. **277**(38): p. 35642-9.
6. Teufel, A., et al., *The longevity assurance homologue of yeast lag1 (Lass) gene family (review).* Int J Mol Med, 2009. **23**(2): p. 135-40.
7. Laviad, E.L., et al., *Characterization of ceramide synthase 2: tissue distribution, substrate specificity, and inhibition by sphingosine 1-phosphate.* J Biol Chem, 2008. **283**(9): p. 5677-84.
8. Mizutani, Y., A. Kihara, and Y. Igarashi, *LASS3 (longevity assurance homologue 3) is a mainly testis-specific (dihydro)ceramide synthase with relatively broad substrate specificity.* Biochem J, 2006. **398**(3): p. 531-8.
9. Rosenthal, E.A., et al., *Linkage and association of phospholipid transfer protein activity to LASS4.* J Lipid Res, 2011. **52**(10): p. 1837-46.
10. Peters, F., et al., *Murine Epidermal Ceramide Synthase 4 Is a Key Regulator of Skin Barrier Homeostasis.* J Invest Dermatol, 2020. **140**(10): p. 1927-1937 e5.
11. Ito, S., et al., *Ceramide synthase 4 is highly expressed in involved skin of patients with atopic dermatitis.* J Eur Acad Dermatol Venereol, 2017. **31**(1): p. 135-141.
12. Riebeling, C., et al., *Two mammalian longevity assurance gene (LAG1) family members, trh1 and trh4, regulate dihydroceramide synthesis using different fatty acyl-CoA donors.* J Biol Chem, 2003. **278**(44): p. 43452-9.
13. Mizutani, Y., A. Kihara, and Y. Igarashi, *Mammalian Lass6 and its related family members regulate synthesis of specific ceramides.* Biochem J, 2005. **390**(Pt 1): p. 263-71.

14. Cadena, D.L., R.C. Kurten, and G.N. Gill, *The product of the MLD gene is a member of the membrane fatty acid desaturase family: overexpression of MLD inhibits EGF receptor biosynthesis.* Biochemistry, 1997. **36**(23): p. 6960-7.
15. Funato, K. and H. Riezman, *Vesicular and nonvesicular transport of ceramide from ER to the Golgi apparatus in yeast.* J Cell Biol, 2001. **155**(6): p. 949-59.
16. Ikeda, A., et al., *Tricalbins Are Required for Non-vesicular Ceramide Transport at ER-Golgi Contacts and Modulate Lipid Droplet Biogenesis.* iScience, 2020. **23**(10): p. 101603.
17. Hanada, K., et al., *CERT and intracellular trafficking of ceramide.* Biochim Biophys Acta, 2007. **1771**(6): p. 644-53.
18. Kitatani, K., J. Idkowiak-Baldys, and Y.A. Hannun, *The sphingolipid salvage pathway in ceramide metabolism and signaling.* Cell Signal, 2008. **20**(6): p. 1010-8.
19. Coant, N., et al., *Ceramidases, roles in sphingolipid metabolism and in health and disease.* Adv Biol Regul, 2017. **63**: p. 122-131.
20. Hatoum, D., et al., *Mammalian sphingosine kinase (SphK) isoenzymes and isoform expression: challenges for SphK as an oncotarget.* Oncotarget, 2017. **8**(22): p. 36898-36929.
21. Gupta, P., et al., *Targeting the Sphingosine Kinase/Sphingosine-1-Phosphate Signaling Axis in Drug Discovery for Cancer Therapy.* Cancers (Basel), 2021. **13**(8).
22. Guitton, J., et al., *Sphingosine-1-Phosphate Metabolism in the Regulation of Obesity/Type 2 Diabetes.* Cells, 2020. **9**(7).
23. White, C., et al., *The emerging role of FTY720 (Fingolimod) in cancer treatment.* Oncotarget, 2016. **7**(17): p. 23106-27.
24. Schnute, M.E., et al., *Modulation of cellular S1P levels with a novel, potent and specific inhibitor of sphingosine kinase-1.* Biochem J, 2012. **444**(1): p. 79-88.
25. Hamada, M., et al., *Induction of autophagy by sphingosine kinase 1 inhibitor PF-543 in head and neck squamous cell carcinoma cells.* Cell Death Discov, 2017. **3**: p. 17047.
26. Sun, M., et al., *Effect of the Sphingosine Kinase 1 Selective Inhibitor, PF543 on Dextran Sodium Sulfate-Induced Colitis in Mice.* DNA Cell Biol, 2019. **38**(11): p. 1338-1345.
27. Shrestha, J., et al., *Synthesis and Biological Evaluation of BODIPY-PF-543.* Molecules, 2019. **24**(23).
28. Park, E.Y., et al., *Synthesis of dansyl labeled sphingosine kinase 1 inhibitor.* Chem Phys Lipids, 2018. **215**: p. 29-33.
29. Hart, P.C., et al., *SPHK1 Is a Novel Target of Metformin in Ovarian Cancer.* Mol Cancer Res, 2019. **17**(4): p. 870-881.
30. Cao, M., et al., *Sphingosine kinase inhibitors: A patent review.* Int J Mol Med, 2018. **41**(5): p. 2450-2460.
31. Wang, J., et al., *Crystal Structure of Sphingosine Kinase 1 with PF-543.* ACS Med Chem Lett, 2014. **5**(12): p. 1329-33.
32. Ju, T., D. Gao, and Z.Y. Fang, *Targeting colorectal cancer cells by a novel sphingosine kinase 1 inhibitor PF-543.* Biochem Biophys Res Commun, 2016. **470**(3): p. 728-734.
33. Ishiyama, M., et al., *A combined assay of cell viability and in vitro cytotoxicity with a highly water-soluble tetrazolium salt, neutral red and crystal violet.* Biol Pharm Bull, 1996. **19**(11): p. 1518-20.
34. Stockert, J.C., et al., *Tetrazolium salts and formazan products in Cell Biology: Viability assessment, fluorescence imaging, and labeling perspectives.* Acta Histochem, 2018. **120**(3): p. 159-167.
35. Park, Y., et al., *Cooperative inhibitory effect of n,n,n-trimethylsphingosine and sphingosine-1-phosphate, co-incorporated in liposomes, on b16 melanoma cell metastasis - cell-membrane signaling as a target in cancer-therapy .4.* Int J Oncol, 1995. **7**(3): p. 487-94.
36. Ohta, H., et al., *A possible role of sphingosine in induction of apoptosis by tumor necrosis factor-alpha in human neutrophils.* FEBS Lett, 1994. **355**(3): p. 267-70.

37. Bonhoure, E., et al., *Overcoming MDR-associated chemoresistance in HL-60 acute myeloid leukemia cells by targeting sphingosine kinase-1.* Leukemia, 2006. **20**(1): p. 95-102.
38. Gao, P., et al., *Characterization of isoenzyme-selective inhibitors of human sphingosine kinases.* PLoS One, 2012. **7**(9): p. e44543.
39. Venant, H., et al., *The Sphingosine Kinase 2 Inhibitor ABC294640 Reduces the Growth of Prostate Cancer Cells and Results in Accumulation of Dihydroceramides In Vitro and In Vivo.* Mol Cancer Ther, 2015. **14**(12): p. 2744-52.
40. Paugh, S.W., et al., *A selective sphingosine kinase 1 inhibitor integrates multiple molecular therapeutic targets in human leukemia.* Blood, 2008. **112**(4): p. 1382-91.
41. Liu, K., et al., *Biological characterization of 3-(2-amino-ethyl)-5-[3-(4-butoxyl-phenyl)-propylidene]-thiazolidine-2,4-dione (K145) as a selective sphingosine kinase-2 inhibitor and anticancer agent.* PLoS One, 2013. **8**(2): p. e56471.
42. Cingolani, F., et al., *Inhibition of dihydroceramide desaturase activity by the sphingosine kinase inhibitor SKI II.* J Lipid Res, 2014. **55**(8): p. 1711-20.
43. Abdel Hadi, L., et al., *Sphingosine Kinase 2 and Ceramide Transport as Key Targets of the Natural Flavonoid Luteolin to Induce Apoptosis in Colon Cancer Cells.* PLoS One, 2015. **10**(11): p. e0143384.
44. Kroll, A., H.E. Cho, and M.H. Kang, *Antineoplastic Agents Targeting Sphingolipid Pathways.* Front Oncol, 2020. **10**: p. 833.
45. Rutti, M.F., et al., *An improved method to determine serine palmitoyltransferase activity.* J Lipid Res, 2009. **50**(6): p. 1237-44.
46. Kim, H.J., et al., *A fluorescent assay for ceramide synthase activity.* J Lipid Res, 2012. **53**(8): p. 1701-7.